

Article

Energy and Exergy Analyses of a Combined Power Cycle Using the Organic Rankine Cycle and the Cold Energy of Liquefied Natural Gas

Ho Yong Lee ¹ and Kyoung Hoon Kim ^{2,*}

¹ Department of Mechanical Engineering, Dongguk University, 30 Pil Dong-Ro 1-Gil, Jung-Gu, Seoul 100-715, Korea; E-Mail: hoyong@dongguk.edu

² Department of Mechanical Engineering, Kumoh National Institute of Technology, 61 Daehak-ro, Gumi, Gyeongbuk 730-701, Korea

* Author to whom correspondence should be addressed; E-Mail: khkim@kumoh.ac.kr; Tel.: +82-54-478-7292; Fax: +82-54-478-7319.

Academic Editor: Kevin H. Knuth

Received: 6 July 2015 / Accepted: 17 September 2015 / Published: 18 September 2015

Abstract: In this work, energy and exergy analyses are carried out for a combined cycle consisting of an organic Rankine cycle (ORC) and a liquefied natural gas (LNG) Rankine cycle for the recovery of low-grade heat sources and LNG cold energy. The effects of the turbine inlet pressure and the working fluid on the system performance are theoretically investigated. A modified temperature-enthalpy diagram is proposed, which can be useful to see the characteristics of the combined cycle, as well as the temperature distributions in the heat exchangers. Results show that the thermal efficiency increases with an increasing turbine inlet pressure and critical temperature of the working fluid. However, the exergy efficiency has a peak value with respect to the turbine inlet pressure, and the maximum exergy efficiency and the corresponding optimum turbine inlet pressure are significantly influenced by the selection of the working fluid. The exergy destruction at the condenser is generally the greatest among the exergy destruction components of the system.

Keywords: organic Rankine cycle (ORC); liquefied natural gas (LNG); low-grade heat source; power generation; exergy

1. Introduction

Natural gas (NG) is a widely-used form of conventional fossil fuel with high levels of energy production and low greenhouse emission problems. Its share in the global energy market shows a stable growing tendency, and it is considered to be the most prospective energy source in forthcoming decades. The disadvantage is that it is in a gaseous state under ambient temperature and pressure, so it usually must be liquefied to liquefied natural gas (LNG) for long-distance transportation and storage, because the energy density of LNG is approximately 600-times greater than that of NG [1,2]. The production of one ton of LNG by liquefying NG requires approximately 850 kWh of electric energy, and regasification also consumes energy [3]. Kumar *et al.* presented an overview of the characteristics of LNG, the present state of affairs of LNG, the eco-friendliness of NG fuel and the potential of NG production from different sources [4].

LNG is stored at a cryogenic temperature of approximately -165°C and at a pressure marginally above atmospheric. Since LNG has a very low temperature, it contains a great amount of cold exergy. Cold exergy of LNG can be extracted in several ways, such as in the process of liquefaction and air separation, in the food industry for storing and freezing foods and in seawater desalination. However, in recent years, the most widely-studied application to exploit LNG exergy is that of improving power cycle efficiency using LNG as a heat sink and as a contributor of additional exergy. When a low-grade heat source is used for the power cycle, the Rankine cycle is considered most suitable. In a power plant based on the Rankine cycle, the LNG cold exergy is used for cooling the condenser. During the process of LNG regasification, the thermal exergy released during vaporization and the heating of NG is used to condense the working fluid. Low temperature condensation can improve cycle efficiency due to the decrease in turbine backpressure [5].

In the power cycle based on the Rankine cycle, using a zeotropic mixture instead of a pure substance as the working fluid has some thermodynamic merits. This is because the evaporation process takes place with variable temperature at a constant pressure, which reduces the exergy destruction in the heat exchanger. A mixture of ammonia and water is commonly used as a working fluid [6]. Miyazaki *et al.* [7] compared the conventional refuse incineration power cycle with the combined power cycle consisting of ammonia-water and LNG Rankine cycles. Lu and Wang [8] proposed a cascading power cycle with LNG expanding directly, consisting of an ammonia-water Rankine cycle and a power cycle of combustion gas to recover the cryogenic energy of LNG. Shi and Che [9] and Wang *et al.* [10] studied a combined cycle of ammonia-water and LNG Rankine cycles using a separator of the ammonia-water mixture. Wang *et al.* [11] analyzed the optimal performance of an ammonia-water Rankine cycle with LNG as a heat sink. Kim *et al.* [12,13] carried out a parametric energy and exergy analysis study for a combined cycle of ammonia-water and LNG Rankine cycles to examine the effects of key system parameters on the system performance.

The organic Rankine cycle (ORC) has been proven to be one of the most feasible methods to achieve high efficiency in low-grade heat recovery. ORC has become a field of intense research in recent years [14–18] owing to its adaptability to various heat sources, proven mature technology, lesser complexity and lesser maintenance, the possibility of small scales, distributed generation systems, low investments, good market availability and well-known market suppliers [19]. Recently, Bao and Zhao reported a review of working fluid and expander selections for the organic Rankine cycle [20], and

Lecompte *et al.* reviewed the ORC architectures for waste heat recovery [21]. Szargut and Szczygiel [22] analyzed the possibilities of the utilization of the cryogenic exergy of LNG for electricity production without any additional combustion of any LNG part with three variants of the plant. Choi *et al.* [23] proposed and investigated a cascade Rankine cycle that consisted of multiple stages of ORC and recovered LNG cold energy for power generation. They presented a review of previous studies on power generation cycles using cold energy sources. Rao *et al.* [24] studied a combined cycle that consisted of the ORC and the LNG Rankine cycles using solar energy as a low-temperature heat source. Kamalinejad *et al.* [25] introduced a mixed integer non-linear programming (MINLP) model to select the optimal synthesis of refrigeration systems to reduce both operating and capital costs of an LNG plant. Soffiato *et al.* [26] investigated ORC to exploit the low-grade waste heat rejected by a ship power generation plant-driven LNG carrier.

Xue *et al.* [27] conducted an analysis of a two-stage ORC with the low-grade heat of the exhaust flue gas of a gas-steam combined cycle power-generating unit, as well as the cryogenic energy of LNG. R227ea and R116 are selected as working fluids for the system. Sun *et al.* [28] proposed a Rankine cycle that uses a mixture of three hydrocarbons as the working fluid to utilize the cold energy in LNG. They showed that while the cycle is relatively simple, a high efficiency can be achieved, and ethylene is most appropriate for the application in the mixed working fluid. Lee *et al.* [29] studied an ORC that uses an R601-R23-R14 ternary mixture as its working fluid and is integrated with a steam cycle as a bottoming cycle and LNG as the cold sink of the working fluid. Kim *et al.* [30] analyzed a cascade power generation system that utilized the cold exergy of LNG and adopted binary working fluids for each stage to minimize the exergy destroyed in the condensers of each stage of the cycle. The review of previous studies on power generation using LNG cold energy is summarized in Table 1 [23].

Table 1. Summary of previous investigations on power generation combined with cold energy recovery.

reference	year	cycle description	fluids	heat source temperature
Miyazaki <i>et al.</i> [7]	2000	Rankine cycle with DEC	NH ₃ -H ₂ O	950 °C
Lu and Wang [8]	2009	Rankine/Brayton cycles/DEC	NH ₃ -H ₂ O	990 °C
Shi and Che [9]	2009	Rankine cycle with DEC	NH ₃ -H ₂ O	157–197 °C
Wang <i>et al.</i> [10]	2013	Rankine cycle with DEC	NH ₃ -H ₂ O	200 °C
Wang <i>et al.</i> [11]	2013	Rankine cycle	NH ₃ -H ₂ O	200 °C
Kim <i>et al.</i> [12,13]	2014/2015	Rankine cycle with DEC	NH ₃ -H ₂ O	200 °C
Czargut and Szczygiel [22]	2009	cascade Rankine cycle	C ₂ H ₆ , C ₃ H ₈	15 °C
Choi <i>et al.</i> [23]	2013	cascade Rankine cycle	C ₂ H ₄ , C ₂ H ₆	15 °C
Sun <i>et al.</i> [28]	2014	ORC with/without DEC	zeotropic	30 °C
Lee <i>et al.</i> [29]	2014	ORC with CO ₂ capture	ternary	87.7 °C
Kim <i>et al.</i> [30]	2015	cascade ORC	binary	25 °C
Soffiato <i>et al.</i> [26]	2015	ORC with career engine	6 fluids	76 °C
Xue <i>et al.</i> [27]	2015	cascade ORC	R227ea, R116	120 °C

Exergy analysis is a powerful and effective tool for designing and analyzing energy systems by combining the conservation of mass and energy principles with the second law of thermodynamics [31]. This study performed energetic and exergetic analyses of a combined power cycle consisting of ORC

and LNG Rankine cycles, where LNG is used to produce power output, as well as to condense the working fluid of ORC as a heat sink. This work focuses on the effects of key system parameters, such as the turbine inlet pressure and the selection of the working fluid, on the system performance, including net power production, thermal and exergy efficiencies and exergy destructions at various components of the system.

2. Methods

A schematic diagram of the combined cycle, consisting of the ORC and the LNG power generation cycle by direct expansion (“LNG cycle”), is shown in Figure 1. In ORC, the working fluid is compressed in Pump 1 from a saturated liquid state (State 1) to a compressed liquid state (State 2). The fluid is then heated in the evaporator using the sensible heat from the source fluid to a saturated or superheated vapor state (State 3). After the mechanical energy is obtained (State 4) owing to the expansion process in Turbine 1, the flow enters the condenser and exchanges heat with the LNG, then returns to State 1. In the LNG cycle, the LNG is supplied from a reservoir as a saturated liquid (State 5) and is pressurized in Feed Pump 2 to a compressed liquid (State 6). It is then heated and vaporized in the condenser to an NG vapor state (State 7), whereby mechanical energy is also extracted in Turbine 2 by the expansion process (State 8). On the other hand, the source fluid enters the evaporator at temperature T_s (State 9) and leaves at temperature T_{sout} after heating the working fluid (State 10).

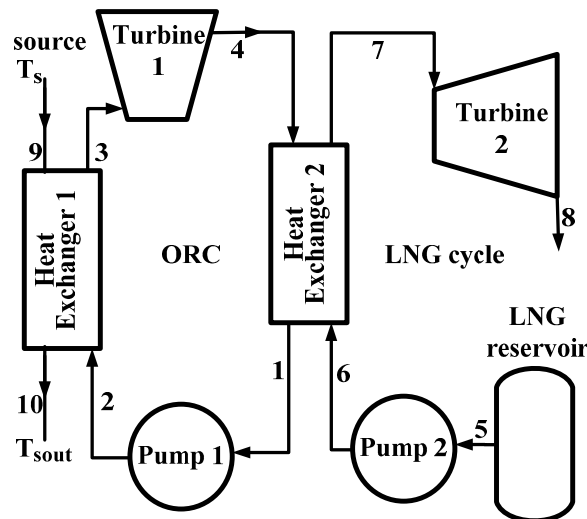


Figure 1. Schematic diagram of the system.

3. System Analysis

The assumptions made for the proposed system analysis include the facts that the flow is steady and that all components are well insulated. Additionally, the LNG is assumed to be pure methane; the fluid is in a pure vapor form at the turbine inlet; and the performances of the pumps or turbines are characterized by constant isentropic efficiencies. The turbine inlet pressure is lower than the critical pressure of the working fluid, so the cycle is limited to a subcritical one. Each of the heat exchangers is assumed to be operated with a pinch point condition, which means that the minimum temperature difference between the hot and cold streams in the heat exchanger reach the prescribed value of the

pinch temperature difference. The pinch point condition indicates the operation with the maximum possible mass flow rate of the working fluid in the evaporator for a given mass flow rate of source fluid and the minimum possible mass flow rate of LNG in the condenser for a given mass flow rate of the working fluid [5,21].

For a specified mass flow rate of the source fluid m_s , the mass flow rate of the working fluid m_w in the ORC and the LNG mass flow rate m_c in the LNG cycle can be determined from the energy balances at the evaporator and condenser as follows [12]:

$$m_w = \frac{m_s c_s (T_9 - T_{10})}{h_3 - h_2} \quad (1)$$

$$m_c = \frac{m_w (h_4 - h_1)}{h_7 - h_6} \quad (2)$$

where c_s is the specific heat of source fluid and h is the specific enthalpy of the working fluid. The numbers used in equations refer to Figure 1. The heat addition rate to the system (Q_{in}), the net power productions of ORC (W_{n1}), the LNG cycle (W_{n2}) and the combined system (W_{net}), can then be evaluated in accordance to the following equations:

$$Q_{in} = m_s c_s (T_9 - T_{10}) = m_w (h_3 - h_2) \quad (3)$$

$$W_{n1} = m_w (h_3 - h_4) - m_w (h_2 - h_1) \quad (4)$$

$$W_{n2} = m_c (h_7 - h_8) - m_c (h_6 - h_5) \quad (5)$$

$$W_{net} = W_{n1} + W_{n2} \quad (6)$$

The heat transfer capability can reflect to a certain degree the heat transfer area of the heat exchanger. The total heat transfer capability of the combined system, UA_{tot} , can be described as follows [18]:

$$UA_{tot} = \frac{Q_{HX1}}{\Delta T_{m,HX1}} + \frac{Q_{HX2}}{\Delta T_{m,HX2}} \quad (7)$$

where Q is the heat transfer rate and ΔT_m is the logarithmic mean temperature difference in the heat exchangers, which is expressed as:

$$\Delta T_m = \frac{\Delta T_{max} - \Delta T_{min}}{\ln(\Delta T_{max}/\Delta T_{min})} \quad (8)$$

The thermal efficiency of the system η_{th} , based on the first law of thermodynamics is defined as the ratio of the net power production to the heat input rate to the system, as follows:

$$\eta_{th} = W_{net} / Q_{in} \quad (9)$$

The definition of the thermal efficiency is based only on the amount of the heat input and the work output. On the other hand, exergy is a measure of the maximum capacity of a system to perform useful work as it proceeds to a specified final state in equilibrium with its surroundings. Exergy is generally not conserved as energy, but destructed in the system. Exergy destruction is the measure of irreversibility that is the source of performance loss [31]. Therefore, an exergy analysis assessing the

magnitude of exergy destruction identifies the location, the magnitude and the source of thermodynamic inefficiencies and can be the basis of the economic analysis of a thermal system [32,33]. The specific exergy is defined as:

$$e = h - h_0 - T_0(s - s_0) \quad (10)$$

where s is the specific entropy and the subscript 0 denotes the dead state. The specific exergy of source fluid at temperature T can be evaluated approximately in accordance to the following equation:

$$e = c_s [T - T_0 - T_0 \ln(T/T_0)] \quad (11)$$

The total exergy input, E_{in} , is determined as the sum of the exergy input to the system by the source fluid $E_s = m_s e_9$ and by the LNG $E_c = m_c e_5$, and it should be equal to the sum of the net power production and the total exergy destruction, including exergy losses, d_{tot} , as:

$$E_{in} = E_s + E_c = W_{net} + d_{tot} \quad (12)$$

The exergy efficiency, η_{ex} , is defined as the ratio of the net power production to the total exergy input of the system. Let us define D to be the exergy destruction ratio of a component as the ratio of the exergy destruction of the component to the total exergy input. The sum of the exergy destruction ratios of the system and the exergy efficiency then become unity [13]:

$$\eta_{ex} = W_{net} / E_{in} = (W_{n1} + W_{n2}) / E_{in} = \eta_{ex1} + \eta_{ex2} \quad (13)$$

$$\eta_{ex} + D_{SE} + D_{LE} + D_{HX1} + D_{HX2} + D_{Wn1} + D_{Wn2} = 1 \quad (14)$$

where η_{ex1} and η_{ex2} are the exergy efficiencies of the ORC and LNG cycles, respectively, and D_{SE} , D_{LE} , D_{HX1} , D_{HX2} , D_{Wn1} , and D_{Wn2} are the exergy destruction ratios of the source fluid exit, LNG exit, evaporator, condenser, turbine and pump in ORC and turbine and pump in the LNG cycle, respectively. The mathematical expressions of the exergy destruction ratios are listed in Table 2.

Table 2. Mathematical expressions of the exergy destruction ratios.

Symbol	Component	Expression
D_{SE}	source exhaust	$m_s e_{10} / E_{in}$
D_{LE}	LNG exhaust	$m_c e_8 / E_{in}$
D_{HX1}	heat exchanger 1	$[m_s(e_9 - e_{10}) + m_w(e_2 - e_3)] / E_{in}$
D_{HX2}	heat exchanger 2	$[m_w(e_4 - e_1) + m_c(e_6 - e_7)] / E_{in}$
D_{Wn1}	net power of ORC	$[m_w(e_3 - e_4 + e_1 - e_2) - W_{n1}] / E_{in}$
D_{Wn2}	net power of LNG cycle	$[m_c(e_5 - e_6 + e_7 - e_8) - W_{n2}] / E_{in}$

The working fluid plays a key role in the cycle, so it must possess physical properties that respond to the Rankine cycle application and an adequate chemical stability in the desired temperature range. The fluid selection criteria are based on the operating conditions, environmental impact, toxicity and flammability level, system efficiency and economic viability [5]. Considering the property of condensing at low temperatures and thermal stability at high temperatures, eight fluids of R22, R134a, R152a, propane, isobutane, R245fa, R123 and isopentane were selected. However, R22 was also

included as a reference, even though it is being currently phased out due to the environmental impact, since it has been widely used and shows excellent power production. In this work, the thermodynamic properties of the working fluids are calculated by the Patel–Teja equation of state [34,35] with MathCAD programming. The basic data of the fluids are shown in Table 3, where M , T_{cr} , P_{cr} and ω are the molecular weight, critical temperature, critical pressure and acentric factor, respectively [36]. Figure 2 shows the temperature-entropy diagrams of the working fluids (a) and of the Rankine cycle with R245fa (b).

Table 3. Basic thermodynamic data of working fluids.

Substance	M (kg/kmol)	T_{cr} (K)	P_{cr} (bar)	ω
R22	86.468	369.30	49.71	0.219
R134a	102.031	380.00	36.90	0.239
R152a	66.051	386.60	44.99	0.263
propane	44.096	396.82	42.49	0.152
isobutane	58.123	408.14	36.48	0.177
R245fa	134.048	427.20	36.40	0.3724
R123	136.467	456.90	36.74	0.282
isopentane	72.150	460.43	33.81	0.228

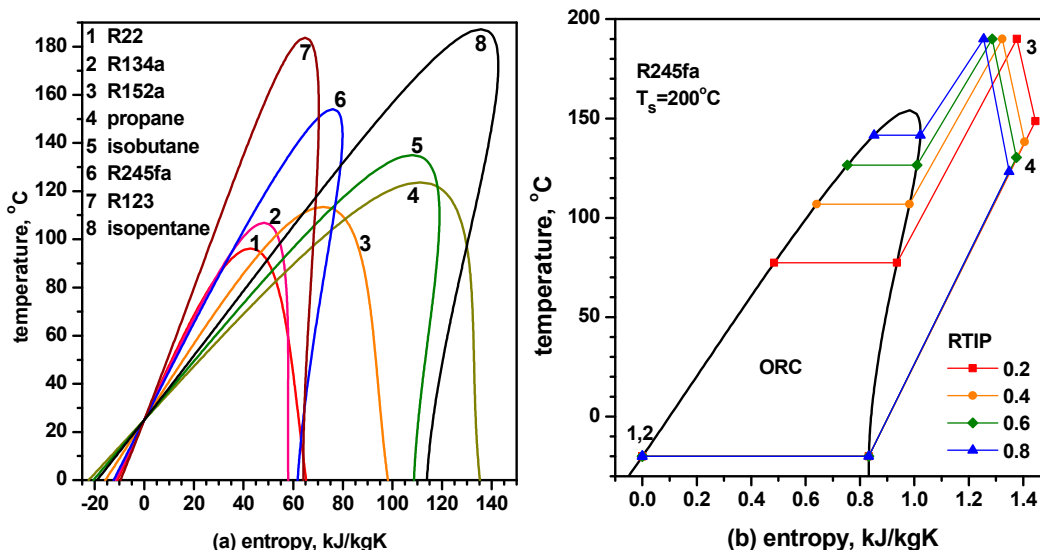


Figure 2. (a) Temperature-entropy diagram of the working fluids; (b) ORC with R245fa.

4. Results and Discussion

4.1. Energy Analysis

In this study, it is assumed that the inlet pressure of Turbine 1 is lower than critical. Therefore, the reduced turbine inlet pressure (RTIP), which is defined as the ratio of the turbine inlet pressure to the critical pressure of the working fluid, is limited to values lower than unity. It is also assumed that the source fluid is standard air with a mass flow rate of 1 kg/s. The input values used as the base case for the cycle simulation are listed in Table 4. Table 5 presents the thermodynamic properties at each point for a typical example using R245fa and RTIP at 0.6 (the turbine inlet pressure is 21.84 bar).

Table 4. Basic simulation conditions of the system.

symbol	description	value	unit
m_s	mass flow rate of source fluid	1	kg/s
T_s	source temperature	200	°C
T_{HI}	turbine inlet temperature	190	°C
T_c	condensation temperature	-20	°C
ΔT_{pp}	pinch temperature difference	8	°C
P_{H2}	LNG turbine inlet pressure	10	bar
P_{L2}	LNG turbine exit pressure	1	atm
η_p	isentropic efficiency of pump	70	%
η_t	isentropic efficiency of turbine	70	%

Table 5. Thermodynamic properties of the working fluids.

No	fluid	x	T (°C)	P (bar)	h (kJ/kg)	s (kJ/kgK)	e (kJ/kg)	m (kg/s)
1	R245fa	0.000	0.0	0.536	0.0	0.000	8.1	0.3005
2	R245fa	-2.161	0.9	21.840	2.1	0.002	9.5	0.3005
3	R245fa	2.167	190.0	21.840	444.6	1.187	99.0	0.3005
4	R245fa	1.875	141.1	0.536	379.6	1.255	13.5	0.3005
5	LNG	0.000	-161.5	1.013	0.0	0.000	1087.8	0.0977
6	LNG	-0.337	-161.0	10.000	3.0	0.008	1088.4	0.0977
7	NG	2.452	133.1	10.000	1170.7	6.264	390.8	0.0977
8	NG	1.750	21.1	1.013	906.1	6.687	0.1	0.0977
9	air	0.000	200.0	0.000	177.8	0.469	37.9	1.0000
10	air	0.000	69.1	0.000	44.8	0.140	3.0	1.0000

In this work, a modified temperature-enthalpy diagram is proposed, where the thermodynamic properties, including the saturated domes of the working fluid and LNG, are evaluated not for the unit mass of the substance, but for the fixed mass flow rate of the source fluid. Then, it may be useful to know the characteristics of the combined cycle, as well as the temperature distributions in the heat exchangers. Figure 3 shows the modified temperature-enthalpy diagrams for (a) R245fa and (b) isopentane at RTIP = 0.6. In the figures, lines 1-2-3 and 9-10 denote the temperatures of the working fluid and source fluid in HX1, and lines 4-1 and 5-6-7 denote the temperatures of working fluid and LNG in HX2. It can be observed that the pinch point in HX1 occurs at the saturated liquid point of working fluid, while the pinch point in HX2 occurs at Point 7. Furthermore, the horizontal distances of lines 3-4 and 7-8 denote the turbine power productions of Turbines 1 and 2, W_{t1} and W_{t2} , respectively.

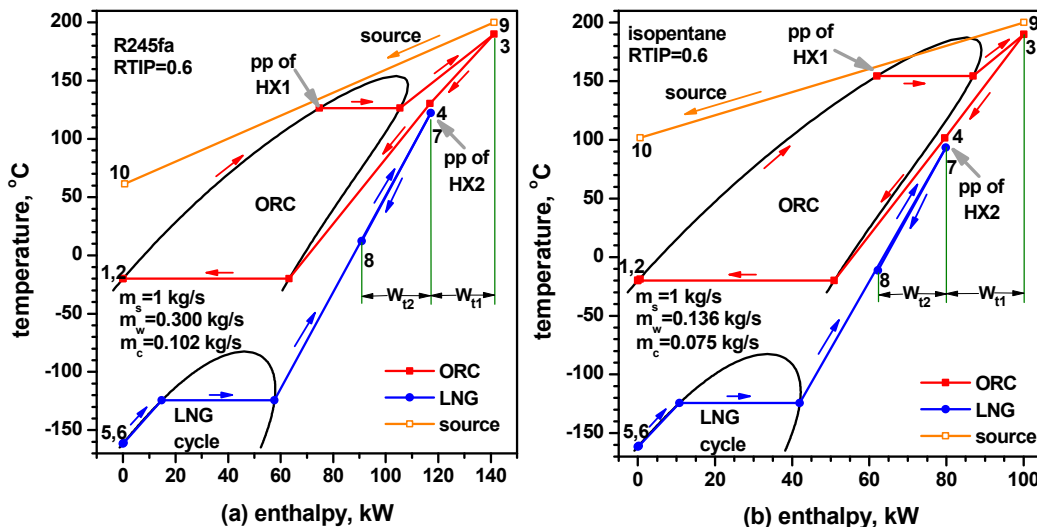


Figure 3. Modified temperature-enthalpy diagrams of (a) R245fa and (b) isopentane at RTIP = 0.6.

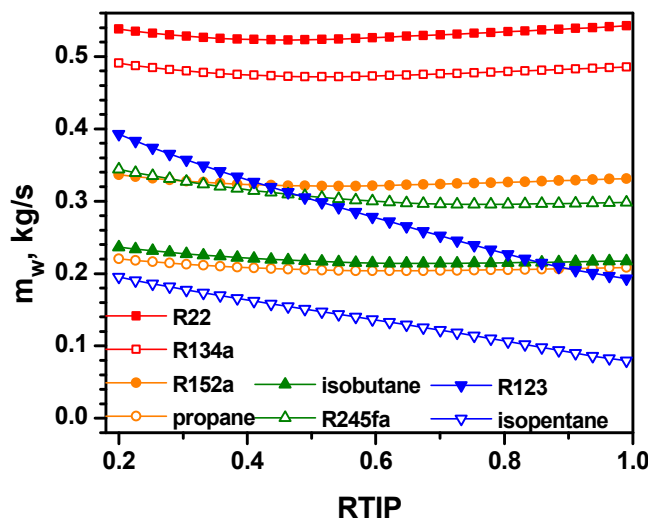


Figure 4. Effects of turbine inlet pressure on the mass flow rate of working fluid for various working fluids.

Figure 4 displays the effects of RTIP on the mass flow rate of the working fluid in ORC for the various working fluids. For working fluids with lower critical temperatures, such as R22, R134a, R152a, propane, isobutane and R245fa, it can be seen from the figure that as RTIP increases, the mass flow rate decreases, reaches a minimum value and then increases again. This can be explained as follows. The mass flow rate is proportional to the temperature drop of the source fluid and inversely proportional to the specific heat of the working fluid added in the evaporator, as is seen in Equation (1). When RTIP is low, an increase in RTIP leads to an elevated evaporation temperature and, consequently, to a higher exit temperature of the source fluid, which acts as a decreasing factor for the mass flow rate with respect to RTIP. When RTIP is high, however, an increase in RTIP leads to a lower specific heat value, which plays a dominant role in increasing mass flow rate with respect to RTIP. The value of RTIP for the minimum mass flow rate increases with increasing critical temperature of the working fluid. The values of RTIP are 0.46, 0.52, 0.54, 0.62, 0.67 and 0.75 for R22,

R134a, R152a, propane, isobutane and R245fa, respectively. On the other hand, the mass flow rate decreases remarkably with increasing RTIP for working fluids at a higher critical temperature, such as R123 or isopentane. This is because the difference between the critical temperature and the source temperature is small, which causes that the decreasing factor for the mass flow rate to play a predominant role compared to the increasing factors.

The net power production of ORC is shown in Figure 5 as a function of RTIP for various working fluids. It can be seen from the figure that the net power increases with increasing RTIP for working fluids with lower critical temperatures. This is because an increase in RTIP leads to an increase in the pressure ratio of the ORC turbine and, consequently, to an increase in the specific ORC turbine work. However, the increasing rate of net power decreases as the critical temperature of the working fluid increases. On the other hand, for the working fluids with higher critical temperatures, such as R123 or isopentane, the power production simply decreases with increasing RTIP, mainly owing to the decreasing mass flow rate.

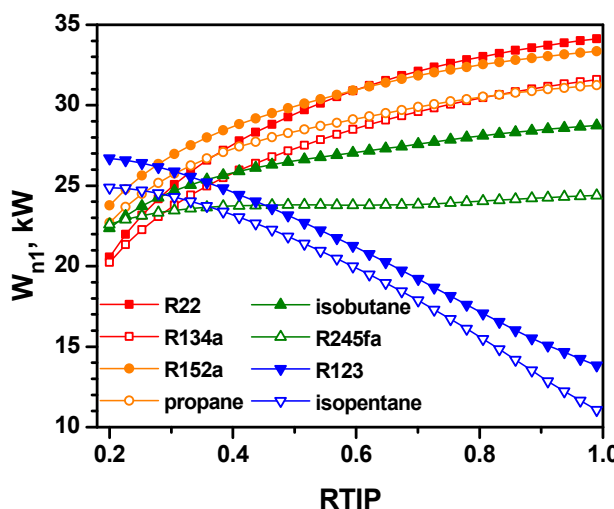


Figure 5. Effects of turbine inlet pressure on the power production in ORC for various working fluids.

The net power production of the LNG cycle and the combined system are plotted against RTIP in Figures 6 and 7, respectively. The net power production of the LNG cycle decreases with increasing RTIP. This is because the temperature at the ORC turbine exit drops with increasing RTIP, which results in a reduction of the turbine inlet temperature of the LNG cycle and, consequently, to a reduction of the specific turbine work of the LNG cycle. It can be seen from the figure that the total net power production generally increases with a decreasing critical temperature of the working fluid. Furthermore, as RTIP increases, it leads to increases in the cases of R22, R134a and R152a, where the critical temperature is relatively low. It is maintained at a nearly constant level for propane and isobutane, for which the critical temperature is kept at middle levels, and leads to decreases for R245fa, R123 and isopentane, for which the critical temperature is relatively high compared to the source fluid.

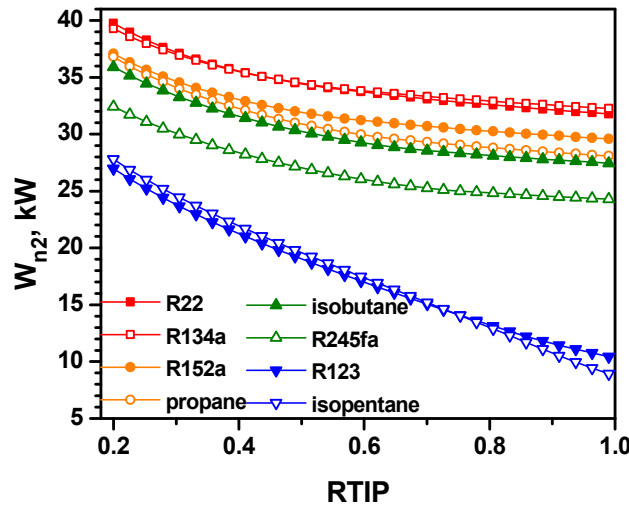


Figure 6. Effects of turbine inlet pressure on the power production in the LNG cycle for various working fluids.

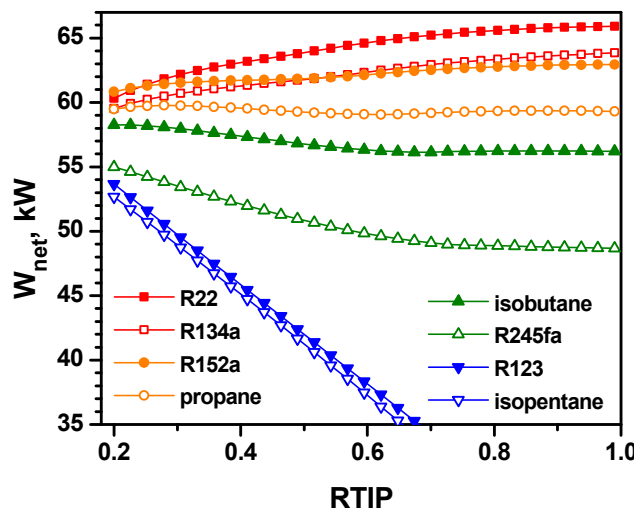


Figure 7. Effects of turbine inlet pressure on the total net power production for various working fluids.

The heat input rate, thermal efficiency and heat transfer capacity of the system, are plotted against RTIP in Figures 8, 9 and 10, respectively. The heat input rate is evaluated as the product of the mass flow rate of the working fluid and the specific heat input at the evaporator. It decreases with increasing RTIP, owing to the decrease in the vaporization heat of the working fluid at an increasing pressure. The thermal efficiency monotonically increases with increasing RTIP, owing to the decreased heat input rate with respect to RTIP. The heat transfer capability UA_{tot} defined in Equation (7) can reflect approximately the heat transfer area and expenditure of heat exchangers. Figure 9 shows that the heat transfer capability generally decreases with increasing RTIP or with the critical temperature of the working fluid. When the source temperature is 200 °C, the maximum thermal efficiencies of ammonia-water-based Rankine with and without the direct expansion cycle of LNG are about 34% and 26% [10,11], respectively, which are higher than all of the results of the thermal efficiencies of working fluids shown in Figure 9.

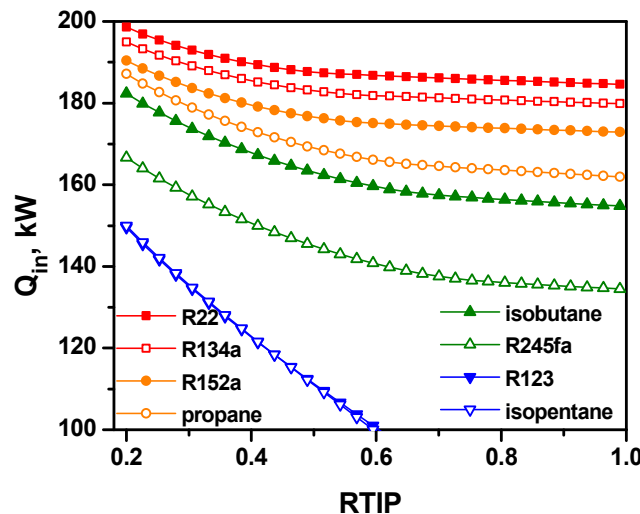


Figure 8. Effects of turbine inlet pressure on the heat input rate for various working fluids.

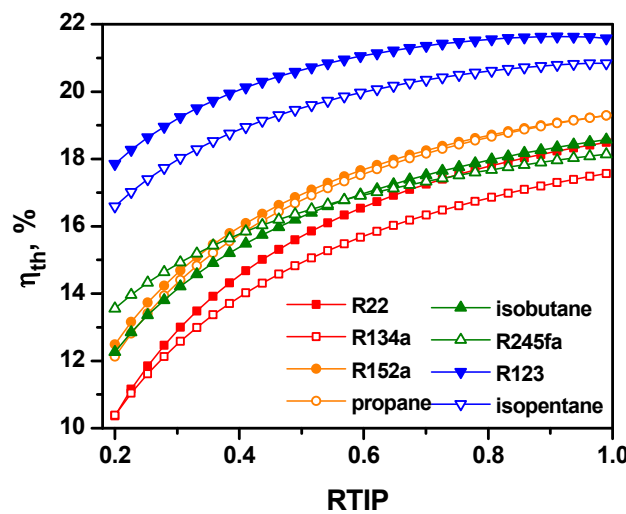


Figure 9. Effects of turbine inlet pressure on the thermal efficiency for various working fluids.

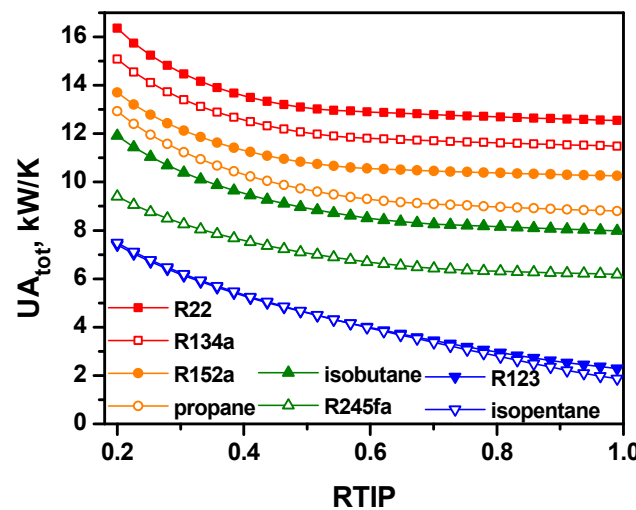


Figure 10. Effects of turbine inlet pressure on the heat transfer capacity for various working fluids.

4.2. Exergy Analysis

Exergy is defined as the maximum theoretical work obtainable from a system in disequilibrium with the reference environment. The dead state is understood as a simple compressible system whose conditions are kept constant and uniform at a pressure of P_0 and temperature T_0 [31]. In this work, they are considered to be $T_0 = 25^\circ\text{C}$ and $P_0 = 1 \text{ atm}$. The total exergy input is the sum of the exergy input with the source fluid and the LNG. The example listed in Table 4 indicates that the specific exergy of the source fluid is 37.9 kJ/kg, whereas the specific exergy of LNG from the reservoir is 1087.8 kJ/kg, which is much greater in value than that of the source fluid. As the mass flow rates of source and LNG are 1 kg/s and 0.0977 kg/s, respectively, the source, LNG and the total exergy input rates are 37.9 kW, 106.3 kW and 144.2 kW, respectively.

Figure 11 shows the effects of RTIP on the total exergy input for various working fluids. For the specified input conditions of the source, the LNG and the mass flow rate of the source fluid, the exergy input rate varies linearly with respect to the mass flow rate of the LNG. As the critical temperature of the working fluid increases, the variation of the exergy input rate owing to the RTIP increases. It can be observed from the figure that the total exergy input rate has a local minimum value with respect to RTIP. The RTIP for the minimum value increases with increases in the critical temperature. The values of RTIP are 0.49, 0.57, 0.57, 0.67, 0.83 and 0.96 for R22, R134a, R152a, propane, isobutane and R245fa, respectively. For the working fluids with a high critical temperature, such as R123 and isopentane, the total exergy input rate decreases monotonically with increasing RTIP, due to monotonically decreasing mass flow rate of working fluid and, consequently, the monotonically decreasing mass flow rate of LNG.

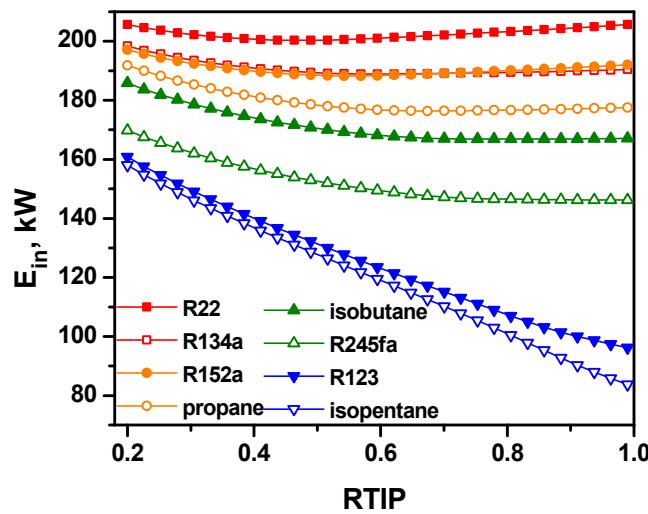


Figure 11. Effects of turbine inlet pressure on the exergy input rate for various working fluids.

The exergy efficiency is illustrated in Figure 12 with respect to RTIP for various working fluids. It can be seen from the figure that the thermal efficiency monotonically increases with increasing RTIP, but the exergy efficiency exhibits a peak with respect to RTIP. The maximum exergy efficiency and the corresponding optimum RTIP depend on the selection of the working fluid. The maximum exergy

efficiencies and the corresponding optimum turbine inlet pressures for working fluids are listed in Table 6.

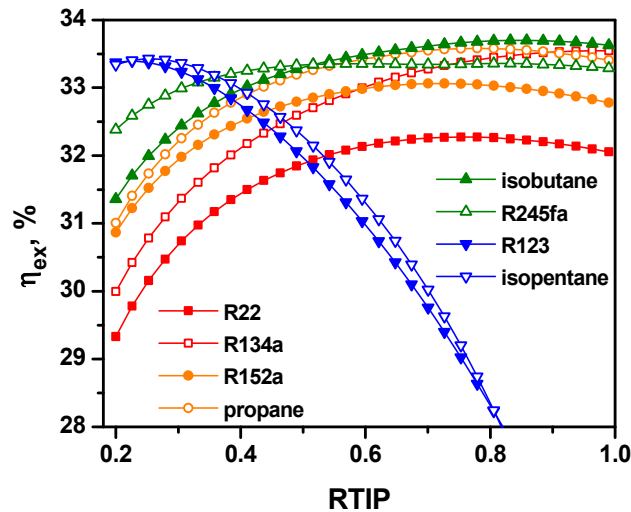


Figure 12. Effects of turbine inlet pressure on the exergy efficiency for various working fluids.

Table 6. Maximum exergy efficiencies and corresponding turbine inlet pressures for working fluids

fluid	maximum exergy efficiency, %	RTIP	TIP, bar
R22	32.2	0.75	37.3
R134a	33.5	0.99	36.5
R152a	33.1	0.73	32.8
propane	33.6	0.78	33.1
isobutane	33.7	0.85	31.0
R245fa	33.3	0.58	21.1
R123	33.4	0.23	8.5
isopentane	33.4	0.25	8.5

Therefore, the maximum efficiencies of propane and isobutane are high, but the corresponding optimal RTIP are high. On the other hand, the maximum efficiencies of R123 and isopentane are slightly lower than those of propane and isobutane, but the corresponding optimal RTIP are low. It is worth noting that the net power production for R22 is the highest among the fluids, but the exergy efficiency, as well as the thermal efficiency is the lowest. If there is no power production with the cold exergy of LNG, the exergy efficiency might be proportional to the net power production of ORC, and the maximum exergy efficiency of R22 is the highest. When the source temperature is 200 °C, the maximum second law efficiency of the ammonia-water Rankine cycle with DEC was about 63% [10], and the maximum exergy efficiency of ammonia-water Rankine cycle with DEC was about 26% [11]. Therefore, we can see that the maximum exergy efficiencies of the working fluids shown in Figure 12 are lower than [11], but higher than [10].

Since the maximum net power production or maximum thermal efficiency cannot reflect the value of the cold exergy of LNG, the exergy efficiency could be a good criterion for the efficient

performance of the system. However, as is shown in Figure 12 or Table 6, the maximum exergy efficiency is similar no matter which fluid is chosen. Therefore, low turbine inlet pressure or small heat transfer capacity could be recommended as additional criteria for the selection of the optimum working fluid.

The exergy destruction ratios at HX1 (D_{HX1}) and HX2 (D_{HX2}) are shown in Figures 13 and 14, respectively, with respect to RTIP and for various working fluids. It can be seen from the figure that D_{HX1} decreases with increasing RTIP for working fluids at a low critical temperature. Subsequently, D_{HX1} increases with RTIP for the working fluids at high critical temperatures, such as R123 or isopentane. This is because the exergy destruction at the evaporator decreases with increasing RTIP or the critical temperature of the working fluid. However, the exergy input rate decreases more sensitively with increasing critical temperature of the working fluid. On the other hand, D_{HX2} generally decreases with increasing RTIP, owing to the decrease in the heat transfer inside the condenser, and the decreasing rate is very large for R123 or isopentane, which have a relatively large critical temperature.

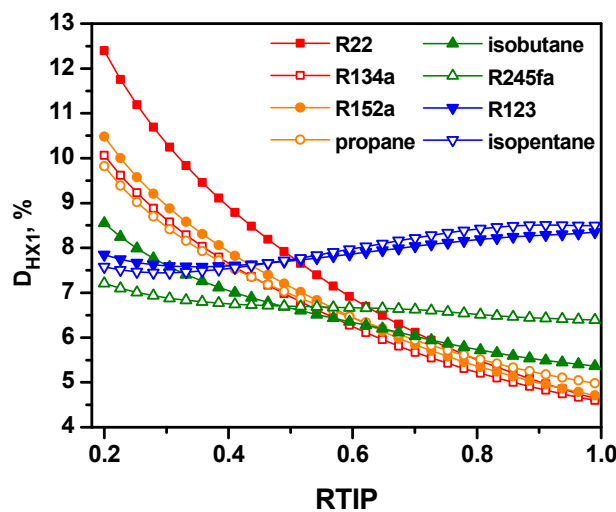


Figure 13. Effects of turbine inlet pressure on D_{HX1} for various working fluids.

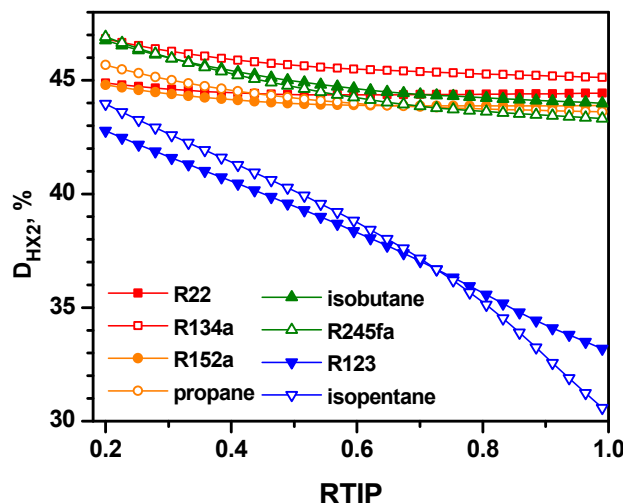


Figure 14. Effects of turbine inlet pressure on D_{HX2} for various working fluids.

Figures 15 and 16 show the (a) normal and the (b) cumulative diagrams of the exergy destruction ratio for each component of the system with respect to RTIP for R245fa and isopentane, respectively. When the working fluid is R245fa, it can be seen from the figure that D_{HX2} is the highest among all of the exergy destruction ratios, and D_{Wn2} and D_{HX1} are higher compared to the others. As RTIP increases, D_{HX2} and D_{Wn2} decrease, while D_{Wn1} and D_{SE} increase; however, the variation owing to RTIP is insignificant. When the working fluid is isopentane, the highest exergy destruction ratio is also D_{HX2} . However, as RTIP increases, D_{HX2} decreases steeply from 44.0% at an RTIP value of 0.2 to 30.6% at an RTIP value of 0.99, while D_{SE} increases steeply from 0.7% at an RTIP value of 0.2 to 24.1% at an RTIP value of 0.99. In this work, the exergy destruction ratio of the condenser D_{HX2} is the highest among others over the entire range of simulation conditions, which indicates that it would be most important to reduce the exergy destruction at the condenser in order to improve the system performance. The diagrams for working fluids with lower critical temperatures, such as R22, R134a, R152a, propane and isobutane, are similar to that of R245fa. Additionally, the diagram for R123 is similar to that of isopentane.

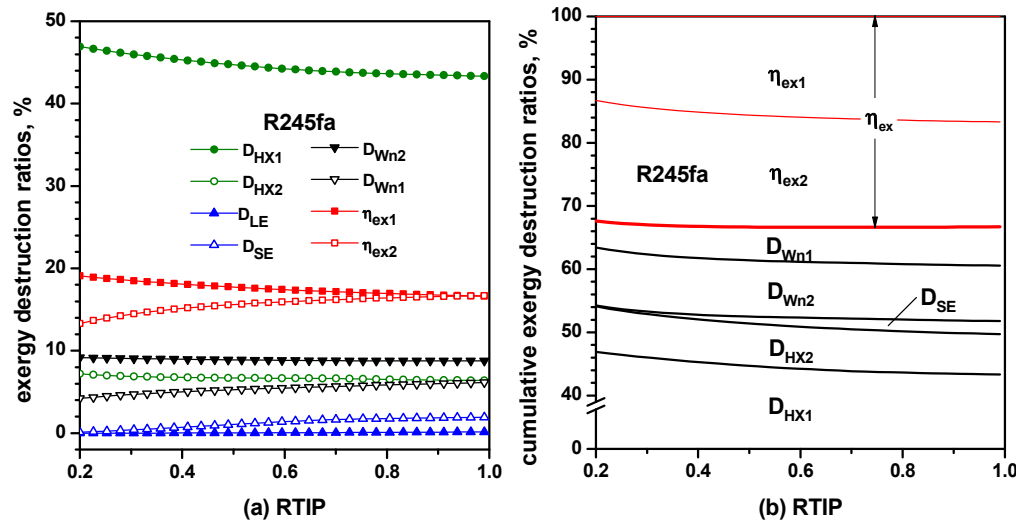


Figure 15. Effects of turbine inlet pressure on the (a) normal and (b) cumulative exergy destruction ratios for R245fa.

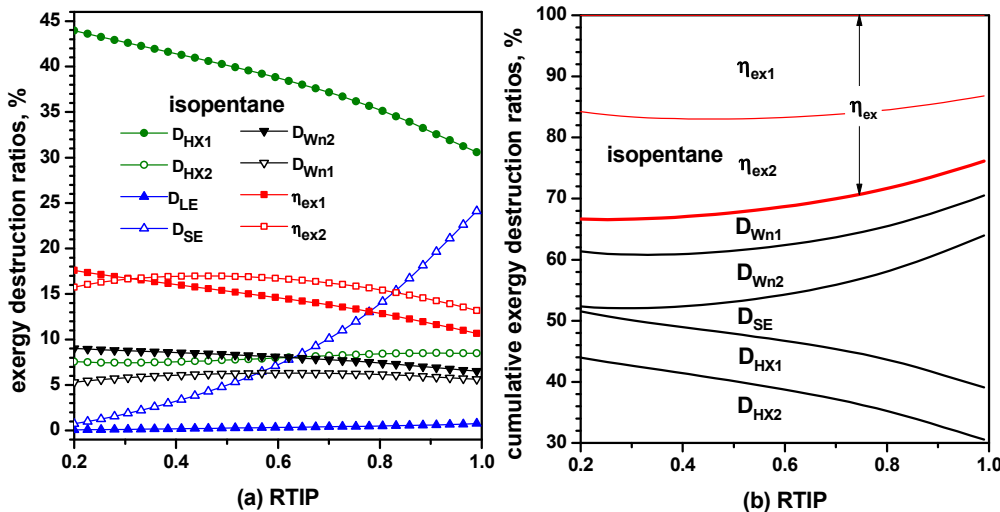


Figure 16. Effects of turbine inlet pressure on the (a) normal and (b) cumulative exergy destruction ratios for isopentane.

5. Conclusions

This paper presents an energetic and exergetic analysis of a combined cycle consisting of an organic Rankine cycle and an LNG Rankine cycle for the recovery of low-grade heat source and LNG cold energy. Air at 200 °C with 1 kg/s is assumed to be the heat source, and eight fluids of R22, R134a, R152a, propane, isobutane, R245fa, R123 and isopentane are considered as the working fluids. The parametric study is carried out with respect to reduced turbine inlet pressure (RTIP) for the different working fluids.

The results show that the power productions of the ORC and LNG cycle are the same order of magnitude, which reflects the importance of cold energy of LNG. As RTIP increases, the power production of the system increases for R22, R134a and R152, but it maintains at a nearly constant value for propane and butane and decreases for R245fa, R123 and isopentane. However, the thermal efficiency increases with increasing RTIP for all working fluids. As the critical temperature of the working fluid increases for a fixed RTIP, the power production shows a decreasing tendency, but the thermal efficiency does the opposite. Therefore, R22 shows the maximum power production of the system, but the minimum thermal efficiency, and *vice versa* for R123 or isopentane.

The exergy efficiency could be more appropriate for the performance criterion of the combined system, since it can account for the effects of the cold energy of LNG. However, the maximum exergy efficiency is similar no matter which fluid is chosen. Therefore, low turbine inlet pressure or small heat transfer capacity could be recommended as additional criteria for the selection of the optimum working fluid. Isopentane or R123 is recommended as the best working fluid, since their maximum exergy efficiency is high and the optimum RTIP and the heat transfer capability are low. The exergy destruction ratios of each component are also examined. Results show that the exergy destruction ratio of the Heat Exchanger 2 is the highest among others over the entire range of the defined simulation conditions. In order to improve the exergetic performance of the system, it is firstly required to reduce the exergy destruction in the Heat Exchanger 2. Therefore, further studies for the cascade Rankine cycles or Rankine cycle with a zeotropic mixture of refrigerants are necessary.

Acknowledgments

This research was supported by the Basic Science Research Program through the National Research Foundation of Korea (NRF) funded by the Ministry of Education, Science and Technology (No. 2010-0007355).

Author Contributions

Dr. Lee suggested and wrote this paper, and Dr. Kim simulated and revised the paper.

Conflicts of Interest

The author declares no conflicts of interest.

Nomenclature

c_p	isobaric specific heat, kJ/kg·K
D	exergy destruction ratio
DEC	direct expansion cycle of LNG
d_{tot}	total exergy destruction, kW
E	exergy flow, kW
e	specific exergy, kJ/kg·K
E_{in}	exergy input rate, kW
h	specific enthalpy, kJ/kg
m	mass flow rate, kg/s
P	pressure, bar
Q	heat transfer rate, kW
RTIP	reduced turbine inlet pressure of Turbine 1
s	specific entropy, kJ/kg·K
T	temperature, °C or K
T_c	critical temperature, °C
T_{cd}	condensing temperature, °C
T_{HI}	turbine inlet temperature of Turbine 1, °C
T_s	source temperature, °C
TIP	turbine inlet pressure of Turbine 1, bar
W_{n1}	net power production of ORC, kW
W_{n2}	net power production of the LNG cycle, kW
W_{net}	net power production, kW
UA_{tot}	total heat transfer capacity of heat exchangers, kW/ °C
ΔT_m	logarithmic temperature difference of a heat exchanger, °C
ΔT_{pp}	pinch temperature difference, °C
η	isentropic efficiency
η_{ex}	exergetic efficiency
η_{th}	thermal efficiency

Subscripts

0	reference state for thermodynamic properties
1	ORC
2	LNG cycle
c	condensation
cr	critical point of working fluid
LE	LNG exhaust
p	pump
s	source
SE	source exhaust
t	turbine
w	working fluid

References

1. Wood, D.A. A review and outlook for the global LNG trade. *J. Nat. Gas Sci. Eng.* **2012**, *9*, 16–27.
2. Roszak, E.A.; Chorowski, M. Exergy analysis of combined simultaneous Liquid Natural Gas vaporization and Adsorbed Natural Gas cooling. *Fuel* **2013**, *111*, 755–762.
3. Liu, H.; You, L. Characteristics and applications of the cold heat exergy of liquefied natural gas. *Energy Convers. Manag.* **1999**, *40*, 1515–1525.
4. Kumar, S.; Kwon, H.T.; Choi, K.H.; Lim, W.S.; Cho, J.H.; Tak, K.J.; Moon, I. LNG: An eco-friendly cryogenic fuel for sustainable development. *Appl. Energy* **2011**, *88*, 4264–4273.
5. Gómez, M.R.; Garcia, R.F.; Gómez, J.R.; Carril, J.C. Review of thermal cycles exploiting the exergy of liquefied natural gas in the regasification process. *Renew. Sustain. Energy Rev.* **2014**, *38*, 781–795.
6. Kim, K.H.; Ko, H.J.; Kim, K. Assessment of pinch point characteristics in heat exchangers and condensers of ammonia-water based power cycles. *Appl. Energy* **2014**, *113*, 970–981.
7. Miyazaki, T.; Kang, Y.T.; Akisawa, A.; Kashiwagi, T. A combined power cycle using refuse incineration and LNG cold energy. *Energy* **2000**, *25*, 639–655.
8. Lu, T.; Wang, K.S. Analysis and optimization of a cascading power cycle with liquefied natural gas (LNG) cold energy recovery. *Appl. Therm. Eng.* **2009**, *29*, 1478–1484.
9. Shi, X.; Che, D. A combined power cycle utilizing low-temperature waste heat and LNG cold energy. *Energy* **2009**, *50*, 567–575.
10. Wang, H.; Shi, X.; Che, D. Thermodynamic optimization of the operating parameters for a combined power cycle utilizing low-temperature waste heat and LNG cold energy. *Appl. Therm. Eng.* **2013**, *59*, 490–497.
11. Wang, J.; Yan, Z.; Wang, M. Thermodynamic analysis and optimization of an ammonia-water power system with LNG (liquefied natural gas) as its heat sink. *Energy* **2013**, *50*, 513–522.
12. Kim, K.H.; Kim, K.C. Thermodynamic performance analysis of a combined power cycle using low grade heat source and LNG cold energy. *Appl. Therm. Eng.* **2014**, *70*, 50–60.
13. Kim, K.C.; Ha, J.M.; Kim, K.H. Exergy Analysis of a Combined Power Cycle Using Low Grade Heat Source and LNG Cold Energy. *Int. J. Exergy* **2015**, *17*, 374–400.
14. Dai, Y.; Wang, J.; Gao, L. Parametric optimization and comparative study of organic Rankine cycle (ORC) for low grade waste heat recovery. *Energy Convers. Manag.* **2009**, *50*, 576–582.
15. Heberle, F.; Brueggemann, D. Exergy based fluid selection for a geothermal organic Rankine cycle for combined heat and power generation. *Appl. Therm. Eng.* **2010**, *30*, 1326–1332.
16. Hung, T.C.; Wang, S.K.; Kuo, C.H.; Pei, B.S.; Tsai, K.F. A study of organic working fluids on system efficiency of an ORC using low-grade energy sources. *Energy* **2010**, *35*, 1403–1411.
17. Uusitalo, A.; Honkatukia, J.; Turunen-Saaresti, T.; Larjola, J. A thermodynamic analysis of waste heat recovery from reciprocating engine power plants by means of Organic Rankine Cycles. *Appl. Therm. Eng.* **2014**, *70*, 33–41.
18. Kim, K.H.; Perez-Blanco, H. Performance Analysis of a Combined Organic Rankine Cycle and Vapor Compression Cycle for Power and Refrigeration Cogeneration. *Appl. Therm. Eng.* **2015**, in press.

19. Tchanche, B.F.; Pétrissans, M.; Papadakis, G. Heat resources and organic Rankine cycle machines. *Renew. Sustain. Energy Rev.* **2014**, *39*, 1185–1199.
20. Bao, J.; Zhao, L. A review of working fluid and expander selections for organic Rankine cycle. *Renew. Sustain. Energy Rev.* **2013**, *24*, 325–342.
21. Lecompte, S.; Huisseune, H.; van den Broek, M.; Vanslambrouck, B.; De Paepe, M. Review of organic Rankine cycle (ORC) architectures for waste heat recovery. *Renew. Sustain. Energy Rev.* **2015**, *47*, 448–461.
22. Szargut, J.; Szczygiel, I. Utilization of the cryogenic exergy of liquid natural gas (LNG) for the production of electricity. *Energy* **2009**, *34*, 827–837.
23. Choi, I.H.; Lee, S.I.; Seo, Y.T. Analysis and optimization of cascade Rankine cycle for liquefied natural gas cold energy recovery. *Energy* **2013**, *61*, 179–195.
24. Rao, W.J.; Zhao, L.J.; Liu, C.; Zhang, M.G. A combined cycle utilizing LNG and low-temperature solar energy. *Appl. Therm. Eng.* **2013**, *60*, 51–60.
25. Kamalinejad, M.; Amidpour, M.; Naeynian, S.M.M. Thermodynamic design of a cascade refrigeration system of liquefied natural gas by applying mixed integer non-linear programming. *Chinese J. Chem. Eng.* **2015**, *23*, 998–1008.
26. Soffiato, M.; Frangopoulos, C. A.; Manente, G.; Rech, S.; Lazzaretto, A. Design optimization of ORC systems for waste heat recovery on board a LNG carrier. *Energy Convers. Manag.* **2015**, *92*, 523–534.
27. Xue, X.; Guo, C.; Du, X.; Yang, L.; Yang, Y. Thermodynamic analysis and optimization of a two-stage organic Rankine cycle for liquefied natural gas cryogenic exergy recovery. *Energy* **2015**, *83*, 778–787.
28. Sun, H.; Zhu, H.; Liu, F.; Ding, H. Simulation and optimization of a novel Rankine power cycle for recovering cold energy from liquefied natural gas using a mixed working fluid. *Energy* **2014**, *70*, 317–324.
29. Lee, U.; Kim, K.; Han, C. Design and optimization of multi-component organic rankine cycle using liquefied natural gas cryogenic exergy. *Energy* **2014**, *77*, 520–532.
30. Kim, K.; Lee, U.; Kim, C.; Han, C. Design and optimization of cascade organic Rankine cycle for recovering cryogenic energy from liquefied natural gas using binary working fluid. *Energy* **2015**, *88*, 304–313.
31. Bejan, A. *Advanced Engineering Thermodynamics*, 3rd ed.; John Wiley & Sons: New York, NY, USA, 2006.
32. Safarian, S.; Aramoun, F. Energy and exergy assessments of modified Organic Rankine Cycles (ORCs). *Energy Rep.* **2015**, *1*, 1–7.
33. Khaljani, M.; Saray, R.K.; Bahlouli, K. Comprehensive analysis of energy, exergy and exergo-economic of cogeneration of heat and power in a combined gas turbine and organic Rankine cycle. *Energy Convers. Manag.* **2015**, *97*, 154–7165.
34. Yang, T.; Chen, G.J.; Guo, T.M. Extension of the Wong-Sandler mixing rule to the three-parameter Patel-Teja equation of state: Application up to the near-critical region. *Chem. Eng. J.* **1997**, *67*, 27–36.

35. Gao, J.; Li, L.D.; Zhu, Z.Y.; Ru, S.G. Vapor-liquid equilibria calculation for asymmetric systems using Patel-Teja equation of state with a new mixing rule. *Fluid Phase Equilibria* **2004**, *224*, 213–219.
36. Yaws, C.L. *Chemical Properties Handbook*; McGraw-Hill: New York, NY, USA, 1999.

© 2015 by the authors; licensee MDPI, Basel, Switzerland. This article is an open access article distributed under the terms and conditions of the Creative Commons Attribution license (<http://creativecommons.org/licenses/by/4.0/>).